Hydrological response in the Lower Danube basin to some internal and external climate forcing factors

Ileana Mares[1], Venera Dobrica[1], Crisan Demetrescu[1], Constantin Mares[2]

[1] Institute of Geodynamics, Romanian Academy, Bucharest, Romania
[2] National Institute of Hydrology and Water Management, Bucharest, Romania

Abstract. The present study aims at investigating the influence on the Danube river discharge of natural forcing factors, such as climate parameters, that characterize internal climate variability (temperature, precipitation, atmospheric circulation indices), and external factors, such as the Earth's magnetic field and the solar forcing. We test the validity of the hypothesis that discharge variability is influenced both by internal and external forcing factors. Our analysis was performed separately for each season, for two time periods, 1901-2000 and 1948-2000. We applied developments in empirical orthogonal functions (EOFs), cross correlations with lags between -1 and 15 years, spectral analysis, filters, composite maps. In the analysis of the correlative results, the serial correlation of time series was taken into account.

In case of zero-lag correlations, the most significant results (confidence levels of 95%) for atmospheric variables are related to the predictor that considers the difference between the first principal component (PC1) of temperatures and precipitation (TPP), except for winter season, when the best predictors are the first principal component of the precipitation field (PC1_PP) and the Greenland-Balkan Oscillation index (GBOI). GBOI is a better predictor for precipitation in the Middle and Lower Danube basins, in comparison with the North Atlantic Oscillation index (NAOI).

Significant results, with a confidence level of more than 95%, were obtained for the PC1_PP and TPP during winter/spring, which can be considered good predictors for the spring/summer discharge in the Lower Danube basin.

A significant signature of the geomagnetic index *aa* was obtained for the band-pass filter smoothed data. According to our results, the atmospheric variables are associated with the solar/geomagnetic variability after about 2-3 years from solar maxima and minima. Possible external signals in the terrestrial variables are also revealed by power spectra and composite maps. The former show statistical significant peaks that can be associated with the Quasi-Biennial Oscillation (QBO) influence and with the solar/geomagnetic variability at the 11-year time scale. The composite maps revealed that the solar impact on atmospheric circulation in the middle troposphere during the East phase of QBO is associated with a blocking event over the northern Atlantic and north-western Europe. A geopotential with an opposite distribution occurs during the solar minimum.

Keywords: NAO, GBOI, serial correlation, low and band-pass filter, atmospheric blocking, climate changes, solar/geomagnetic activity, Danube basin

1 Introduction

The climatic system is a closed one, being influenced mainly by external factors, whose action is modulated by internal mechanisms. The main external factors that contribute to the climate variability are the solar activity in its various forms and the greenhouse gases. As shown for instance by Cubasch et al. (1997) and by Benestad and Schmidt (2009), it is difficult to distinguish between the anthropogenic and the solar signals and to assess

separately the climatic system response to their variations, especially when the recent warming comes into discussion, mainly due to limitations of simulation climate models and lack of long time-span data in many parts of the world.

Lohmann et al. (2004) detected solar variations associated with the Schwabe, Hale, and Gleissberg cycles of solar activity in the spatial patterns of sea-surface temperature and sea-level pressure, using band pass filters with frequencies appropriate to each of the solar cycles. Significant correlations between global surface air temperature and solar activity were obtained by Echer et al. (2009), applying wavelet decomposition. Explanation of the physical mechanism of correlations with certain lags between solar activity and climate variables can be found in Gray et al. (2013), Scaife et al. (2013), Thiéblemont et al. (2015).

Recent studies on the impact of solar/geomagnetic activity on the climate are reviewed by Brugnara et al. (2013). After a statistical reconstruction of the main atmospheric fields for more than 250 years, the authors perform an analysis of the 11-year solar signal in different reconstructed terrestrial datasets. They find that there is a robust response of the late-wintertime tropospheric circulation to the sunspot cycle, independently of the data set. This response is particularly significant over Europe. Although many publications reveal solar signal in Earth's climate, by various more or less robust methods, using reconstructed long time series, the scientific community has not reached a consensus on this matter. Among publications criticizing such results and showing the difficulties in highlighting this link and pointing to some errors in these investigations we mention those by Versteegh (2005) and Benestad and Schmidt (2009). The authors of these works describe also the physical mechanisms that should be considered in such investigations. Perry (2007) and Gray et al. (2010) also discussed the possible mechanisms determining the response of the Earth's climate system to solar varibility. Velasco and Mendoza (2008) found that the main indices of atmospheric large-scale circulation show power spectra peaks that can be associated with Schwabe (11-15 years) and Hale (22- 24) solar cycles.

Regarding internal factors that influence climate at regional or local scale, a best known one, which influences climate variability in the Atlantic sector and in Europe, is the North Atlantic Oscillation (NAO) (Hurrell et al., 2003). NAO corresponds to a North-South dipole of the pressure, characterized by opposite sign simultaneous anomalies between temperate and high latitudes over the Atlantic sector. Rimbu et al. (2002) showed that there is an out-of-phase relationship between the time series of the Danube river discharge anomalies and the NAO index (NAOI). Also, Rimbu et al. (2005) found that spring Danube discharge anomalies are significantly related to winter Sea Surface Temperature (SST) anomalies. Mares et al. (2002) found, however, that the NAO signal in climate events in the Danube lower basin is relatively weak in comparison with other regions. On the other hand, NAOI is a significant predictor for Seine river (Massey et al., 2010; El - Janyani et al., 2012), north-eastern Algeria (Turki, et al., 2016), southern Sweden (Drobyshev et al., 2011), northern Italy (Zanchettin et al., 2008). Barriopedro et al. (2008) and Rimbu and Lohmann (2011) found that solar activity plays an essential role in modulating the blocking features with the strongest signal in the Atlantic sector.

The interaction between internal and external factors is extensively studied by Van Loon and Meehl (2014). Recent research (Valty et al., 2015) warns that for the selection of predictors such as NAO, there is a need to consider the dynamics of the total oceanic and hydrological system over wider areas. In fact, the entire climate system needs to be considered. Hertig et al. (2015) discuss the consequences of climate non-stationarities and describe the mechanisms underlying the non-linearity and non-stationarity of the climate system components, with a focus on NAO.

Since the Danube discharge estimation has a great importance for Romania's economy, in the present investigation we focus on predictors for the Lower Danube basin

discharge. The main aim of our work is to select, from various terrestrial and solar/geomagnetic variables, predictors with significant information for that discharge, applying robust tests for the statistical significance. Besides the NAO influence on climate variables in the Danube basin, we analyze the atmospheric index Greenland-Balkan Oscillation (GBOI), introduced by Mares et al. (2013b), which reflects the baric contrast between the Balkan and the Greenland zones. We also consider in this paper the indices of blocking type circulation, both on the Atlantic and European sector, and take into account the effect of the phases of Quasi-Biennial Oscillation (QBO) in the region. The strong serial correlations shown by the solar and geomagnetic variables have been properly taken into account.

This paper is organized as follows: Section 2 presents data processed at regional (2.1) and large (2.2) scale, as well as the indices that define solar and geomagnetic activity (2.3). In Section 3, we describe the methodology. Section 4 discusses the results. Concerning the link between atmospheric circulation at large scale and the climate variables at local or regional scales we demonstrate that GBOI is a more significant predictor than NAOI for the climate variables in the Danube middle and lower basin (4.1). In subsection 4.2, we consider several predictors for climatic variables in the Danube basin, including indices of large-scale atmospheric circulation, for the period 1901-2000, and we test predictor's weight for the discharge in the lower basin. In subsection 4.3, the results obtained from the correlation analysis of solar/geomagnetic signal with terrestrial variables (4.3.1), the lags involved (4.3.2), and the QBO role in modulating these influences (4.3.3), are presented. The conclusions are summarized in Section 5.

2 Data

2.1 Regional scale

The Lower Danube Basin discharge was recorded by Orsova station (ORS_Q), located at the entrance of the Danube in Romania. It represents an integrator of the upper and middle basin. Data were provided by the National Institute of Hydrology and Water Management, Bucharest, Romania.

We performed our analysis separately for each season, for two time series, one of 100 values in the time interval 1901-2000 and the other of 53 values, between 1948 and 2000. For the period 1901-2000, in the Danube upper and middle basin (DUMB), precipitation (PP), mean temperature (T), diurnal temperature range (DTR), maximum and minimum temperatures (Tmx, Tmn), cloud cover (CLD) were considered at 15 meteorological stations upstream of Orsova. The selection of stations was done according to their position on the Danube or on its tributaries (Fig.1).

The monthly values of the above variables were obtained from http://climexp.knmi.nl.

Data-sets are calculated on high-resolution grids (0.5 x 0.5 degree) by the Climatic Research Unit (CRU). In order to obtain the grid point nearest to station, we selected "half grid points".

The seasonal averages for all variables considered in this study have been used.

2.2 Large scale

In order to see the influence of large-scale atmospheric circulation on the variables at the regional scale, we considered the seasonal mean values of the sea level pressure field (SLP) in the sector 50^0W-40^0E, 30^0–65^0N. SLP data were available at http://rda.ucar.edu/datasets/ds010.1 of the National Center for Atmospheric Research

(NCAR). The 5-degree latitude/longitude grids, computed from the daily grids, begin in 1899 and cover the Northern Hemisphere from 15^0N to the North Pole. The accuracy and quality of this data is discussed by Trenberth and Paolino (1980).

The NAO index was downloaded from http://www.ldeo.columbia.edu/res/pi/NAO/.

The GBO index, introduced by Mares et al. (2013b), was calculated using the correlative analysis of the first principal component (PC1) of the Empirical Orthogonal Functions (EOFs) for the precipitation field at the 15 stations of this study with sea level pressure (SLP) at each grid point where it was defined (Fig. 2). Then GBOI is calculated as differences of normalized SLP at Nuuk and Novi Sad, located in opposite sign correlation nuclei of Fig. 2.

For the 1948-2000 time-span we considered blocking type indices, besides the atmospheric variables taken over 1901-2000. The calculation of these indices involves pressure differences between mid-and northern latitudes, as shown below, in the Methods section. For the geopotential at 500 hPa (1948-2000) provided by *British Atmospheric Data Centre (BADC)* (https://badc.nerc.ac.uk/home/index.html).Three sectors were taken into account: Atlantic-European (AE) on the domain (50°W- 40°E; 35°N - 65°N), Atlantic (A) defined in (50°W - 0°, 35°N - 65°N) and European (E) in the region (0° - 40°E; 35°N - 65°N). The corresponding blocking indices are AEBI, AI, EBI, respectively.

2.3 Solar/geomagnetic data

For the 100 years interval 1901-2000, the solar/geomagnetic activities are quantified by the sunspot number, retrieved from ftp://ftp.ngdc.noaa.gov/STP/space-weather/solar-data/solar-indices/sunspot-numbers/ /international and, respectively, by the *aa* index. The latter describes the geomagnetic activity at mid-latitudes; it is available at http://isgi.cetp.ipsl.fr/lesdonne.htm. For the shorter time interval 1948-2000, the solar forcing is quantified by the solar radio flux at 10.7 cm (usually called F10.7 index). Details on the 10.7 cm solar radio flux and its applications are given by Tapping (2013). Since the 10.7 cm solar radio flux is a more objective measurement, and always measured on the same instruments, this proxy for "solar activity" should have a similar behavior but smaller intrinsic scatter than the sunspot number.

The Quasi-Biennal Oscillation (QBO) is also used in this study in order to make the link between solar forcing, internal climate variability and discharge variability.

The QBO values were downloaded from http://www.geo.fu-berlin.de/met/ag/strat/produkte/qbo/qbo.dat, Free University of Berlin.

3 Methodology

The time series of the variables considered for the 15 stations of the study were developed in empirical orthogonal functions (EOFs) and only the first principal component (PC1) was kept (Mares et al., 2009, 2015a, 2016a). By means of the difference between PC1 of the temperatures (PC1_T) and of precipitation (PC1_PP), both standardized, we get a drought index (TPPI). This is a slightly modified procedure (Mares et al., 1996), based on the Ped's (1975) methodology.

The blocking index (*BI*) at the 500 hPa geopotential field was estimated according to Lejenas and Okland (1983). A blocking event can be identified when the averaged zonal index, computed as the 500 hPa height difference between 40°and 60°N, is negative over 30° in longitude.

We calculated for each longitude λ three indices, for the regions: Atlantic-European (AEBI), Atlantic (ABI) and Europe (EBI) according to:

$$I_B(\lambda) = \Phi(\lambda, 57.50\,N) - \Phi(\lambda, 37.50\,N), \quad (1)$$

where Φ is the 500 hPa geopotential field. The blocking index BI is a mean for λ longitudes of $I_B(\lambda)$. Positive BI reflects a blocking type circulation.

Data filtering

Low-pass filters were applied to the terrestrial fields to eliminate oscillations due to factors such as El Niño–Southern Oscillation (ENSO). The Mann filter (Mann, 2004, 2008) was applied with three variants that eliminate frequencies corresponding to periods lower than 8, 10 and 20 years.

Band pass filters were applied both to the terrestrial and to solar/geomagnetic variables. The band pass filters were of the Butterworth type (Butterworth, 1930), and the variables have been filtered in the 4-8, 9–15 and 17-28 years bands. According to Vlasov et al. (2011) and Ault et al. (2012), the frequency response for these filters is nearly flat within the passband, and they are computationally efficient, being recursive filters.

Correlation analysis

The correlation analysis in case of solar/geomagnetic activity is conducted in this paper for lags between -1 to 15 years. In many investigations, significant solar signal in the terrestrial variables has been obtained applying band-pass filters to isolate the frequency bands of interest (Lohmann et al., 2004; Dima et al., 2005; Prestes et al., 2011; Echer et al., 2012; Wang and Zhao, 2012).

In the present study we apply band pass filters for three frequency bands: (4-8yr), (9-15yr) and (17-28 yr). Because the filtered time series show a strong autocorrelation, to test the statistical significance of the link between the terrestrial and solar variables we use the *t-test*, which takes into account the effective number of independent variables and the correlation coefficient between two series. The effective number is a function of the serial correlations of the two series analyzed. Details about the statistical analysis of hydro-climatic variables can be found in Rai et al. (2013).

Serial correlation

In order to find the significance level of the correlation coefficient, we have to take into account the fact that by smoothing both terrestrial and solar/geomagnetic variables present a serial correlation. Serial correlation (also called autocorrelation) means that there is a correlation between one time series (x_t) and the same series lagged by one or more time units (x_{t+k}). The serial correlation coefficient for k lags (sr_k) is given by:

$$sr_k = \frac{\sum_{t=1}^{N-k}(x_t - \bar{x}_t).(x_{t+k} - \bar{x}_{t+k})}{\left[\sum_{t=1}^{N-k}(x_t - \bar{x}_t)^2.\sum_{t=1}^{N-k}(x_{t+k} - \bar{x}_{t+k})^2\right]^{1/2}}, \quad (2)$$

where N is the sample size.

In the case when the analyzed time series present serial correlation, we have to estimate first the equivalent sample size (ESS). There are several methods to find the statistical significance of correlation among pairs of series presenting serial correlations (e. g., Thiebaux and Zwiers, 1984; Zwiers and von Storch, 1995; Ebisuzaki, 1997). Mares et al.

(2013a) applied the procedure described by Zwiers and von Storch (1995) to find ESS in order to estimate the statistical significance of climatic change signal in the sea level pressure field (SLP) in 21st century in comparison with the 20th century.

In the present analysis, in order to find the ESS, namely the number of effectively independent observations (N_{eff}), a simple formula is applied, which is appropriate for the correlations involving smoothed data (Bretherton et al., 1999):

$$N_{eff} = N \frac{(1 - r_1 r_2)}{(1 + r_1 r_2)} \quad , \qquad (3)$$

where r_1 and r_2 are the lag-1 autocorrelation coefficients corresponding to the two correlated time series, and N the number of the observations.

In the next step, the t-statistics (von Storch and Zwiers, 1999), is used to test the statistical significance of the correlation coefficient.

$$t = |r| [(N_{eff} - 2)/(1 - r^2)]^{1/2} \quad , \qquad (4)$$

where r is the correlation coefficient between the two variables and N_{eff} is the effective number used in the testing procedure.

Following von Storch and Zwiers (1999), the null hypothesis $r = 0$ is tested by comparing the t value in equation (4) with the critical values of t distribution with $N_{eff} - 2$ degrees of freedom.

The correlated time series must have a Gaussian distribution. For this reason in the present study we have also computed the nonparametric Kendall correlation coefficient, which measures correlation of ranked data. Applying the algorithm described by Press et al. (1992), correlation values and corresponding significance p-levels are obtained. A comparison between the Pearson and Kendall correlation coefficients is found in Love et al. (2011), where the statistical significance of the correlation between sunspots, geomagnetic activity, and global temperature is tested.

Statistical significance of the amplitude of the time series power spectra

Testing the statistical significance of the spectral peaks resulting from an analysis of a time series is usually done by building a reference spectrum (background) and comparing the amplitude spectrum of the analyzed time series to those of the background noise spectrum. This spectrum is based on either white or most often red noise (Ghil et al. 2002, Torrence and Campo, 1998). All amplitudes above the background noise amplitudes for a given significance level are considered significant at that level. We checked the null hypothesis, which in case of spectral analysis is that the time series has no significant peak and its spectral estimate does not differ from the background noise spectrum. Rejection of the null hypothesis means accepting spectral peaks that exceed a certain level of significance. As shown by Mann and Less (1996), theoretical justifications exist for considering red noise as noise reference (background) for climate and hydrological time series. Also, Allen and Smith (1996) show a first-order autoregressive (AR1) process must be considered for the null hypothesis test, in order that the analysis technique be useful in geophysical applications. If the white noise is considered as the null hypothesis, it might incorrectly indicate a large number of oscillations which are not significant.

The power spectra of this study were estimated by the multitaper method (MTM) (Thomson, 1982; Ghil et al., 2002; Mann and Less, 1996). The MTM procedure is a nonparametric technique that does not a priori require a model for the generation of time

series analysis, while the harmonic spectral analysis assumes that the data generation process includes purely periodic components and white noise which are overlapped (Ghil et al., 2002).

In this study red noise was chosen as reference background spectrum. The significance of spectrum peaks relative to the red noise background is based on the elementary sampling theory (Gilman et al., 1963; Percival and Walden, 1986). Mares et al. (2016a) estimated the background noise and the significance of power spectral peaks in case of the influence of the Palmer drought indices on the Danube discharge.

4 Results and discussion

4.1 Connection between atmospheric circulation at large scale and climate parameters for the study area

The atmospheric circulation at the large scale is quantified in this section by the North Atlantic Oscillation index (NAOI), the Greenland Balkan Oscillation Index (GBOI) and indices that highlight the blocking type circulation, such as the European blocking index (EBI). A first result (Table 1) concerns the correlation between the first principal component (PC1) for precipitation and NAO/GBO indices during winter, calculated for two time intervals, 1916-1957 and 1958-1999. The opposite signs of the correlation coefficients in case of NAO and GBO stem from the way the two indices are defined. The direct impact of NAO is less pronounced than the GBO one for the surrounding areas of the lower Danube basin, confirming previous investigations (Mares et al., 2013b, 2015a,b; 2016a,b). Also, the high correlation between GBOI and precipitation is stable over time, as can be seen from the same table.

In Fig. 3 we compare, for the winter season, the temporal evolution of the first principal component (PC1) for the precipitation in the Danube basin with GBOI, for the time interval 1959-1999; they show a high correlation, with a coefficient of 0.84.

In Fig. 4 the correlation coefficients between winter precipitation at each of the 15 stations of the study and winter NAOI and GBOI for two time intervals, 1916-1957 and 1958-1999, are presented. Except for the first five stations, located in the upper basin of the Danube, the correlation is high, with a stronger GBOI signal compared to the NAO one. The correlation coefficients when the PC1 of precipitation is considered are higher and regard all stations.

4.2 Testing predictor variables for estimating the discharge in the Lower Danube basin (1901-2000)

The contribution to the Danube discharge in the lower basin (at Orsova) of the nine predictors, described in Sections 2 and 3, is shown in Fig. 5 as correlation coefficients between these predictors and the discharge, for each of the four seasons. The 99% confidence level for the correlation coefficients for 100 values is reached for correlation coefficient values in excess in comparison with the critical value of 0.254 (Brooks and Carruthers, 1953). There are many predictors that are statistically significant at this level of confidence, but we take into consideration only those having the highest correlation coefficients. As can be seen from Fig. 5, the drought index (TPPI), that depends on the PC1 of precipitation and temperature, brings the greatest contribution to the Danube discharge in seasons of spring, summer and fall, with correlation coefficients (r) of -0.450, -0.730, -0.700 respectively. In winter season, the precipitation field in the upper and middle basin has the most important contribution to the discharge in lower Danube basin (r = 0.500). The second contribution is of

GBOI (r = 0.430). Also, it can be seen that for the spring season, where contribution of the drought index TPPI is lower than in summer and autumn, the GBOI and DTR can be considered good predictors, with r = 0.420 and, respectively, -0.417.

Considering predictors to the Danube discharge with some anticipation, significant results obtained for an anticipation of a season are presented in Fig. 6. For spring discharge, the best predictor is clearly the winter drought index (r = -0.62). TPPI in spring is a significant predictor (r = -0.55) for summer discharge, along with the spring precipitation field (PC1_PP) (r = -0.53). The highest predictability for the Danube discharge is found in spring, considering TPPI during winter as predictor.

Rimbu et al. (2005) described the winter SST role in the predictability of spring Danube discharge. Ionita et al. (2008) found stable teleconnections between SST, temperature and precipitation during the winter season and the spring Elbe discharge. Our results related to winter NAOI influence on the Danube discharge are in accordance with the ones obtained by Bierkens and van Beek (2009), i. e. NAOI has an influence with a good statistical significance, but we found that GBOI is better, especially for the Lower Danube basin.

Fig. 7 shows the spring Orsova discharge (standardized) in comparison with EBI and GBOI for winter in the time interval 1948-2000. For this period, a good correlation is also found in case of winter GBOI (R = 0.53) and the atmospheric circulation of blocking type, quantified by the European blocking index EBI (r = -0.54), as predictors to the spring Danube discharge at Orsova.

The opposite signs of the Orsova discharge correlations with EBI and GBOI are due to the way the two indices are defined. The negative correlations between discharge and EBI can be explained as follows. As shown by Davini et al. (2012), the midlatitude traditional blocking localized over Europe, uniformly present in a band ranging from the Azores to Scandinavia, leads to a relatively high pressure field in most of Europe. This field of high pressure, that is not favorable for precipitation, defines a positive blocking index, and leads to low Danube discharge at Orsova. A positive correlation coefficient between the Danube discharge at Orsova and GBOI means that a positive GBO index leads to a low pressure in the Danube basin area and therefore to a high discharge. The role of the atmospheric circulation of blocking type on hydrological events in the Danube Basin is described in several investigations, Blöschl et al. (2013) and Mares et al. (2015b). Lorenzo-Lacruz et al. (2011) review the investigations on the interaction between river discharges and low-frequency climate patterns; the authors specify that several studies have demonstrated the occurrence of teleconnection patterns affecting the European climates, particularly in winter.

In the present study, the best predictor for the Danube discharge is found to be the drought index TPPI, which is a simple index, easy to calculate. This index stores also effects of SST or other phenomena at large scale such as ENSO or GBO on the temperature and precipitation fields.

The results obtained in the present study are consistent with those of Mares et al. (2016a), where the Palmer drought indices were found as good predictors for the discharge in the lower basin. Papadimitriou et al. (2016) analyze the changes in future drought climatology for five major European basins (including Danube) and estimate the impact of global warming.

4.3 Solar/geomagnetic signature in the climate fields in Danube basin

As a solar activity indicator we used the sunspot number for the interval 1901-2000 and the 10.7 cm solar radio flux for the time interval 1948-2000. Although the solar flux is closely correlated with sunspot numbers, these values are not identical, the correlation coefficient varying with the season (0.98-0.99). The geomagnetic activity was quantified by

the *aa* index for both time intervals. Regarding the link between solar and geomagnetic activity, details can be found in Demetrescu and Dobrica (2008).

The solar/geomagnetic signal was tested by correlative analyses (cross correlation with lags between -1 to 15 years) composite maps and spectral analyses. Prior to the correlative analysis, data were filtered using low- and band-pass filters for the terrestrial variables and only band-pass filters for the solar/geomagnetic indices.

4.3.1 Zero-lag correlation analysis

Results that have a higher than, or at least a 95% confidence level are given in Table 2, for the analysis time-span of 100 years (1901-2000). Since not all variables have a normal distribution, the Kendall's coefficient was associated to Pearson's coefficient. There were cases when the difference between the two correlation coefficients was relatively high, probably due to the statistical distribution that deviates from normal. Therefore, the significant correlation indicated by the Pearson coefficient (r) is analyzed together with the Kendall correlation coefficient (τ) and their levels of significance (p).

Three categories of data have been considered: non-filtered (UF), smoothed by low pass filtering (LPF) to eliminate periods less than, or equal to 8 years, only for terrestrial variables, and band pass filter (BPF) applied to both terrestrial and solar/geomagnetic indices. Lines in bold face mean there are at least two situations for the same season (filtered or unfiltered data) having a significant correlation coefficient (CL).

As can be seen from Table 2, smoothing time series led to improved correlation coefficients; the most significant results were obtained by band-pass filters with frequency corresponding to 9-15 yr. Tests were performed also for 17-28 yr band-pass filters, resulting the highest correlation coefficients. However, because the effective number is very small (about 5 years) due to the very high serial correlation caused by such filters, we consider that for that kind of band-pass filters much larger sets of data are necessary. Reducing the number of effective observations when smoothing is applied is discussed in Palamara and Bryant (2004), where they test the statistical significance of the relationship between geomagnetic activity and the Northern Annular Mode.

Highest correlations with *aa* were obtained during the summer season for temperature (r = 0.796) and for precipitation (r = - 0.721), for a smoothing by a 9-15yr BPF. Also, in summer, it is worth mentioning the *aa* influence on the drought index (TPPI), with a correlation coefficient of 0.787, for a 9-15 yr filtering. It can be noted that TPPI responds better to the *aa* signal, compared to PC1_PP.

Regarding solar activity signature in temperatures and precipitation, the highest correlation coefficients were found for the fall season (0.699) and, respectively, for spring (-0.538) in the filter band 9-15 yr. Correlations with the sunspot number having a particularly high confidence level (> 99%) are observed in the case of 4-8 yr band smoothed time series, such as the atmospheric circulation index GBOI (summer and winter).

The results obtained in the present investigation, referring to the temperature and precipitation variables, are in general accordance with results of Dobrica et al. (2009; 2012), which analyzed long time series (100–150 years) of temperature and precipitation annual means from records of 14 meteorological stations in Romania. The correlations with the geomagnetic *aa* index and the sunspot number have the same sign, i. e. positive for temperatures and negative for precipitation, in spite of rather different areas of investigation (but subject to the same large-scale atmospheric circulation), smoothing procedure and separate analysis for individual seasons.

Taking into account both possible signals, of the geomagnetic and of solar activity, we can notice that during spring TPPI has the best response for unfiltered or filtered time series. The unfiltered time series for *aa* and sunspot number are presented in Fig. 8, in comparison

with TPPI for 1901-2000. The solar flux from 1948 is also plotted. Correlation coefficients between TPPI and *aa*, and TPPI and sunspot number are 0.275 and respectively 0.211, with a confidence levels of 99% and 95% (Table 2 for TPPI (UF)).

As regards the solar/geomagnetic signals in the Danube discharge at Orsova, we found that *aa* is associated with the discharge (ORS_Q), with highest significance during the summer season (r = -0.656). However, considering our criterion to have significant correlations in at least two cases, the fall data, for which the smoothing by LPF and BPF (9-15) also show a significant association with *aa,* are of interest.

In the following, some results obtained for the time interval 1948-2000, for which the blocking type circulation indices and the 10.7 cm solar flux are available, are given in Table 3. We note that due to short time series, of only 53 years, although the smoothing by the band pass filter 9-15 yr leads to correlation coefficients with high confidence level, the number of degrees of freedom is quite small in this case. The smoothing by a 4-8 yr BPF appears most appropriate for highlighting a possible solar /geomagnetic signal in the blocking indices, with an intensification of the activity of blocking circulation, when the activity of the external factors increase. Considering the aa index influence on the blocking indices, the most significant relationship is obtained for the European region (EBI), where all statistics leads to a significance higher 99%. A possible influence of solar activity is evidenced during the winter for EBI, and in autumn for ABI and AEBI.

Links between solar / geomagnetic activity, and climate events at large scale such as ENSO, taking into account the periodicities smaller (such as 4 - 8 years) than the well-known 11-year cycle, were found in several investigations including Narasimha and Bhattacharyya (2010) and Sunkar and Tiwari (2016).

4.3.2. Power spectra

The association between solar or geomagnetic variability with the terrestrial climate variability can be signaled out also by estimating periodicities in the climate time series by means of power spectra. In the present study the power spectra were estimated by means of the multitaper method (MTM). Unfiltered time series are used, in order to see whether there is solar/geomagnetic signature in climate data. For the time series of unfiltered European blocking index (EBI) during winter, the power spectra given in Fig. 9a reveal that the most significant periodicity is related to QBO (2.4 years). The peaks at 10.7 and 14.2 years, which may be linked to the 11-year solar/geomagnetic cycle, are determined with an approximately 90% confidence level. In case of spring EBI (Fig. 9b), the only significant peak with a confidence level of 95% corresponds to a period of 10 years. This is consistent with the results shown in Table 3, where during spring, the time series of blocking index EBI, both unfiltered and 4-8 yr band-pass filtered, have significant correlations with the *aa* geomagnetic index. Also, in winter, the possible response of EBI to solar activity quantified by the 10.7 cm solar flux is statistically significant with CL almost 99%. A significant peak related to QBO (Fig. 9c) is found for the spring blocking index over the Atlantic European region (AEBI).

4.3.3 Lagged Correlation Analysis

To see if there is a link with some delay between solar or geomagnetic indices and climate variables considered in this study, we performed correlative analyses with lags from -1 to 15 years. As with the zero-lag correlations, three variable types, i.e. unfiltered, low-pass and band-pass filter smoothed data, have been considered.

For the 1901-2000 time-span, the most significant correlation coefficient (CL> 99%) with the geomagnetic *aa* index was obtained for the 9-15 yr BPF summer drought index TPPI at a lag of 1 (r = 0.885) and 2 years (0.730). In this case, the effective number was 16. This result is supported by the ones obtained in case of LPF smoothing, for which the correlation

coefficients had a CL of 95%, with the effective number 34. Similar results were obtained for the correlation between TPPI and sunspot numbers, with a correlation coefficient slightly lower than in case of *aa*.

A variable that is associated with the solar activity even more significantly than to the geomagnetic index, is the atmospheric circulation index GBO in summer. Fig. 10 is a summary for the three types of time series. The correlation coefficient between the sunspot number and unfiltered GBOI does not show any statistical significance no matter of the lag value. For the LPF smoothed GBO index, the correlation is significant at a lag of 3yr (95%). At this lag, the 9-15 yr BFP time series shows a high statistical significance (CL ~ 99%). Accordingly, in the summer, at 2-3 years after a maximum (minimum) of solar activity, a diminution of GBO index is possible, i. e. a decrease (increase) of atmospheric pressure in Greenland area and an increase (decrease) of the pressure in the Balkans might happen.

A possible response of the atmospheric circulation index GBOI to solar variability with a delay of 2-3 years, is due to the ocean-atmosphere interactions, as described by Thiéblemont et al. (2015), who analyzed the solar signal in NAOI. The authors propose a new synchronization mechanism that combines air–sea interaction processes and solar-induced stratospheric dynamics modulation to simulate the observed solar influences on North Atlantic climate, using a coupled ocean-atmosphere model under two versions. The results obtained in this paper based only on statistical methods, are in accordance with the ones reported by Thiéblemont et al. (2015), as the most significant link between NAOI and solar flux is found for lags betwen 1 and 3 years, with correlation coefficients of around 0.6, for the 9-13 years band pass filtered data. The correlation coefficients between solar flux and GBOI in Fig. 10 are negative, due to GBOI definition in comparison with the NAOI. Zanchettin et al. (2008) demontrate the NAO role in the modulation of the link between Sun and discharges in the northen Italy.

Regarding the time interval of 53 years (1948-2000), significant links between the solar activity quantified by the 10.7 cm solar flux and the Danube discharge at Orsova were obtained for spring and summer, with different lags. With a delay of 2 years, both unfiltered and filtered time series of the Danube discharge indicate statistically significant correlations with solar flux.

Like in the GBOI case, the discharge is oppositely, but well correlated with solar activity at some lags. In Fig. 11a, correlation coefficients are shown at lags between -1 and 15 yr, for unfiltered (UF), low pass filter (LPF), and 9-15 yr band pass filter smoothed time series. It can be noticed that, if for the unfiltered data the correlation is significant (95%) at lags of 1, 2 and 3 yr, for BPF smoothed data, the significance is situated between 95-99% at lags of 2, 3, and 4 yr. Taking into account the LPF smoothed discharge, the most significant correlation (90%) is obtained when the taken discharge values have delays of 2 and 3 years from the solar flux.

In Fig. 11b the coherent time evolutions of the solar flux and of the 9-15 yr BPF smoothed discharge, with a lag of 3 years for which the correlation coefficient is highest (-0.769) and CL is 99% have been shown.

From the above results, we can expect that at 2 or 3 years after a maximum (minimum) solar activity, the spring discharge to be lower (higher). In Fig. 11c, the power spectra for the Danube discharge during spring indicates significant peaks at 4 yr (CL close to 95%) and at 10.7 yr, with a CL near 90%. These peaks might be associated with the internal atmospheric variability and respectively with the solar variability. Peaks of power spectra associated with the solar variability for the discharge in other regions of the world, are found by Tomasino and Valle (2000), Landscheidt (2000), Compagnucci et al. (2014).

Although our results are obtained from relative short time series, they are consistent with results found by Pena et al. (2015). These authors investigated the summer floods in

Switzerland for more than 300 years and concluded that high frequency of flooding is related to solar activity minimum, and that a summer flood damage index shows a significant component with a frequency corresponding to 10-12 years.

A different possible signature of solar activity was found in the time series of the index that defines atmospheric circulation of blocking type over Atlantic-European region, for the period 1948-2000, during the winter season. As can be seen in Fig. 12, a possible response of blocking circulation to the solar activity is given by significant correlations with a delay of 2 and 3 years to the solar flux. It is worth noting that in this case, the filtering process does not lead to an improvement of the significance of the correlation, even if the value of the correlation coefficient increases. Accordingly, we might conclude that about 2-3 years after a maximum (minimum) solar activity, during winter, the atmospheric circulation of the blocking type is enhanced (weakened) over the Atlantic-European region.

4.3.4 QBO role in modulation of the influence of solar forcing

Regarding QBO influence on the relationship between solar activity and terrestrial parameters, there are several investigations (Van Loon and Labitzke, 1988; Bochníček et al.1999, Huth et al., 2009) which demonstrated that the QBO phase is very important for emphasizing these links. We see in QBO mainly an important modulator of the impact of solar activity on lower troposphere processes. To test this hypothesis, in this paper we selected the winter months in years with East QBO phase, and correlations between solar flux and terrestrial variables were calculated.

The correlation coefficient between the solar flux and the unfiltered winter EBI for all those 53 years, is 0.15 and not statistically significant. By selecting only the years with QBO in the East phase in the winter months (34 cases), the correlation coefficient is 0.32 at the confidence level around 95%. It is interesting that although the power spectrum (Fig. 9a) highlights significant peaks related to the QBO (2.4 and 2.7 years), the correlation coefficient between EBI and QBO is insignificant. This suggests that the spectral representation is very useful in time series analysis and the QBO phases modulate the connection between solar activity and blocking circulation. These findings related with the QBO role are in accordance with the results obtained by Barriopedro et al. (2008), Huth et al., (2009), Sfîcă et al. (2015). Cnossen and Lu (2011) presented some of the mechanisms which explain the QBO role in the solar signature in climate variables. These mechanisms have been supported by both observational and modeling studies, but some of them are yet unclear.

Composite maps enlighten the solar impact on atmospheric circulation in the lower troposphere, during the East phase of QBO, when the solar maximum is associated with blocking event over the northern Atlantic and north-western Europe (Fig. 13a), and the solar minimum to a geopotential with an opposite distribution (Fig.13b). Sfîca et al. (2015) specify that through these composite maps nonlinearities are taken into account, at odds to using linear methods. Barriopedro et al. (2008) found similar results, namely QBO is a modulator of the transformation of atmospheric circulation from a blocking type circulation to a zonal one and vice versa, under the solar impact.

We mention that during 1948-2000, 34 winter months (DJF) were recorded in which East QBO phase occurred and the solar flux has produced atmospheric blocking events in the lower troposphere, or a zonal atmospheric circulation at middle and higher latitudes, depending on the state of maximum or minimum solar activity, respectively.

5 Conclusions

In the present investigation, we focused on finding predictors for the discharge in the Lower Danube basin, which present a high level of statistical significance.

In the first part of the paper we tested predictors for the discharge, from the fields of temperature, precipitation, cloud cover in the Danube basin, and indices of atmospheric circulation over the Atlantic-European region. Each of the temperature, precipitation and cloud cover fields in the Danube basin was decomposed in EOFs, and as predictors were considered only the first principal component (PC1). A drought index (TPPI), derived from the standardized PC1 of the temperature and the precipitation, was also taken as predictor for the discharge in the Lower Danube basin.

The atmospheric circulation has been quantified by Greenland-Balkan Oscillation (GBO) and North Atlantic Oscillation (NAO) indices and the blocking type indices. The analysis was performed separately for each season in two time intervals, 1901-2000 and 1948-2000.

The main statistically significant results for this part of our research are the following:

1. The zero-lag correlative analyses for each season revealed that, except for the winter season, the drought index (TPPI) has the highest weight for the discharge variability in the Lower Danube basin;
2. Testing the predictors with a lag of several months in advance of discharge, we concluded that TPPI in winter and spring is a good indicator for the Danube discharge in spring and summer respectively;
3. The winter GBOI has a more significant influence on the climate variables in the Danube middle and lower basin than NAOI;
4. Analysis for the period 1948-2000 reveals that in winter the GBOI weight for the Danube discharge is similar to that of the blocking index over the European sector.

In the second part of the paper, we focused on the solar/geomagnetic impact on the terrestrial variables. Because the solar and geomagnetic variables, as well as the smoothed time series by means of various filters (low-pass and band-pass) applied in this investigation, show strong serial correlations, all correlative analyses were performed through rigorous testing of statistical significance. The number of observations was reduced to the effective number of degrees of freedom, corresponding to independent observations. The main findings of our research for this topic are the following:

5. The most significant signatures of solar/geomagnetic variability were evidenced in the drought indicator (TPPI). Because the precipitation does not respond just as well as temperatures to the solar variability, the analysis of the TPPI variable instead of temperatures and precipitation separately is preferable;
6. From the analysis of correlations with delays of the terrestrial variables in comparison with the solar/geomagnetic activity from -1 to 15 years, we obtained very different results, depending on the season and on the considered variables, as well as on the filtering procedure. Accordingly, we might conclude that in winter, about 2-3 years after a maximum (minimum) solar activity, the atmospheric circulation of blocking type is enhanced (weakened) over the Atlantic-European region. Also, it was found that the Danube discharge in the lower basin, during spring and summer, will be lower (higher) at 2 or 3 years after a solar maximum (minimum);
7. An atmospheric index that is associated with the solar variability is the atmospheric circulation index GBO in summer. At 2-3 years after a maximum (minimum) of solar activity, one can expect a change of atmospheric circulation in the Atlantic-European region, quantified by GBOI, shown by a diminution of this index, i. e. a decrease

(increase) of pressure in Greenland area and an increase (decrease) in atmospheric pressure in the Balkans;

8. The power spectra obtained by the multitaper method (MTM) have highlighted quasi-periodicities related to solar activity and to other oscillations such as QBO. In the time series of AEBI (spring), and EBI (winter) the most significant periodicity is related to QBO (2.2-2.7 years). Also, at an approximately 90% confidence level there are peaks at 10-14 years, which may be linked to the 11-year solar cycle;
9. The composite maps revealed that the solar maximum impact on atmospheric circulation in the middle troposphere during the East phase of QBO is associated with a blocking event over the northern Atlantic and north-western Europe. A geopotential with an opposite distribution occurs during the solar minimum.

In this study, we focused only on observational data, so in our next investigations we shall consider outputs of climate simulation models, from which significant predictors for the Danube basin found in this investigation, like GBOI, TPPI and atmospheric blocking indices, will be calculated and tested.

Acknowledgements. This study has been performed under VALUE: COST Action ES1102. We thank the two anonymous referees for rigorous and constructive comments and suggestions that served to improve this study.

References

Allen, Myles R., and Smith, L. A.: "Monte Carlo SSA: Detecting irregular oscillations in the presence of colored noise.", Journal of Climate 9, no. 12 , 3373-3404, 1996.

Ault, T. R., Cole, J. E., and George S. St.: The amplitude of decadal to multidecadal variability in precipitation simulated by state-of-the-art climate models, Geophysical Research Letters 39, no.21, 2012.

Barriopedro, D., Garcıa-Herrera, R., and Huth, R.: Solar modulation of Northern Hemisphere winter blocking, J. Geophys. Res., 113, D14118, doi: 10.1029/2008JD009789, 2008.

Benestad, R.E.: Schmidt GA: Solar trends and global warming, J. Geophys. Res. 114:D14101, doi: 10.1029/2008JD011639, 2009.

Bierkens, M. F. P. and Van Beek, L. P. H.: Seasonal Predictability of European Discharge: NAO and Hydrological Response Time, J. Hydrometeorol., 10, 953–968, 2009.

Blöschl, G., Nester, T., Komma, J., Parajka, J., and Perdigão, R. A. P.: The June 2013 flood in the Upper Danube Basin, and comparisons with the 2002, 1954 and 1899 floods, Hydrol. Earth Syst. Sci., 17, 5197–5212, doi: 10. 5194/hess -17-5197-2013, 2013.

Bochníček, J., Hejda, P., and Pýcha, J.: The effect of geomagnetic and solar activity on the distribution of controlling pressure formations in the Northern Hemisphere in winter, Studia geophysica et geodaetica, 43(4), 390-398, 1999.

Bretherton, C.S., Widmann, M., Dymnikov, V.P., Wallace, J.M., and Bladé, I.: The effective number of spatial degrees of freedom of a time-varying field, Journal of climate, 12(7), 1990-2009, 1999.

Brooks, C. E. P., and Carruthers, N.:Handbook of statistical methods in meteorology. Her Majesty's Stationery Office, London, 1953, 413 pp. 1953.

Brugnara, Y., Brönnimann, S., Luterbacher, J., and Rozanov, E.: Influence of the sunspot cycle on the Northern Hemisphere wintertime circulation from long upper-air data sets, Atmos, Chem. Phys., 13, 6275-6288, doi:10.5194/acp-13-6275-2013, 2013.

Butterworth, S., On the theory of filter amplifiers, Wireless Engineer, 7, 536-541,1930.

Cnossen, I., and Lu, H.: The vertical connection of the quasi-biennial oscillation-modulated 11 year solar cycle signature in geopotential height and planetary waves during Northern

Hemisphere early winter, J. Geophys. Res., 116, D13101, doi:10.1029/2010JD015427, 2011.

Compagnucci, R. H., Berman, A. L., Herrera, V. V., and Silvestri G.: Are southern South American Rivers linked to the solar variability?. International Journal of Climatology 34, no. 5, 1706-1714, 2014.

Cubasch, U., Voss, R., Hegerl, G.C., Waszkewitz, J. and Crowley, T.J.: Simulation of the influence of solar radiation variations on the global climate with an ocean-atmosphere general circulation model, Climate Dynamics, 13(11), 757-767, 1997.

Davini, P., Cagnazzo, C. Gualdi, S., and Navarra, A.: Bidimensional Diagnostics, Variability, and Trends of Northern Hemisphere Blocking, J. Climate, 25, 6496–6509, 2012.

Demetrescu, C. and Dobrica,V.: Signature of Hale and Gleissberg solar cycles in the geomagnetic activity, J. Geophys. Res., 113, A02103, doi: 10.1029/2007JA012570, 2008.

Dima, M., Lohmann, G., and Dima I.: Solar-Induced And Internal Climate Variability at decadal time scales, Int. J. Climatol., 25: 713–733, 2005.

Dobrica, V., C. Demetrescu, Boroneant, C. and Maris G.: Solar and geomagnetic activity effects on climate at regional and global scales: Case study-Romania, J.Atmos. Sol.-Terr. Phy., 71 (17-18), 1727-1735, doi: 10.1016/j.jastp.2008.03.022, 2009.

Dobrica V, Demetrescu, C.: On the evolution of precipitation in Central and South-Eastern Europe and its relationship with Lower Danube discharge, in: AGU Fall Meeting Abstracts, l 1, 1030, 2012.

Drobyshev, I., Niklasson, M., Linderholm, H.W., Seftigen, K., Hickler, T., Eggertsson, O.: Reconstruction of a regional drought index in southern Sweden since AD 1750, The Holocene 21(4) 667-679, doi: 10.1177/0959683610391312, 2011.

Ebisuzaki, W.: A Method to Estimate the Statistical Significance of a Correlation when the Data is Serially Correlated, J. Climate, 10:2147–2153, 1997.

Echer, M. S., Echer, E., Nordemann, D. J. R., and Rigozo, N. R.: Multi-resolution analysis of global surface air temperature and solar activity relationship, Journal of Atmospheric and Solar-Terrestrial Physics, 71(1), 41-44, 2009.

Echer, M.S., Echer, E., Rigozo, N.R., Brum, C.G.M., Nordemann, D.J.R., and Gonzalez, W.D.: On the relationship between global, hemispheric and latitudinal averaged air surface temperature (GISS time series) and solar activity, Journal of Atmospheric and Solar-Terrestrial Physics, 74, pp.87-9, 2012.

El-Janyani, S., Massei, N., Dupont, J.P., Fournier, M. and Dörfliger, N.: Hydrological responses of the chalk aquifer to the regional climatic signal, Journal of Hydrology, 464, 485-493, 2012.

Ghil, M., Allen, M.R., Dettinger, M.D., Ide, K., Kondrashov, D., Mann, M.E., Robertson, A.W., Saunders, A., Tian, Y., Varadi, F., and Yiou, P.: Advanced spectral methods for climatic time series, Reviews of Geophysics 40 (1), doi: 10.1029/2001RG000092, 2002.

Gilman, D. L., Fuglister, F. J., and Mitchell, J. M. : On the power spectrum of "red noise", J Atmos Sci **20:**182–184, 1963.

Gray L. J., Beer, J., Geller, M., Haigh, J., Lockwood, M., Matthes, K., Cubasch, U., Fleitmann, D., Harrison, G., Hood, L., Luterbacher, J., Meehl, G., Shindell, D., van Geel, B., and White, W.: Solar influences on climate. Reviews of Geophysics, 48: RG4001. DOI: 10.1029/2009RG000282, 2010.

Gray, L. J., Scaife, A. A., Mitchell, D. M., Osprey, S., Ineson, S., Hardiman,S., Butchart, N., Knight, J., Sutton, R., and Kodera K.: A lagged response to the 11 year solar cycle in observed winter Atlantic/Euro pean weather patterns, J. Geophys. Res. Atmos., 118, 13, 405–13, 420, doi: 10.1002/2013JD020062, 2013.

742 Hertig, E., Beck, C., Wanner, H., and Jacobeit, J.: A review of non-stationarities in climate
743 variability of the last century with focus on the North Atlantic-European sector, Earth-
744 Science Reviews 147, 1–17, doi:10.1016/j.earscirev.2015.04.009, 2015.
745 Hurrell, J.W., Kushnir, Y., Visbeck, M., and Ottersen, G.: Research Abstracts EGU2007-A-
746 08910
747 9:1029-2003. An overview of the North Atlantic Oscillation. In: Hurrell, J.W., Kushnir,
748 Y., Ottersen, G., Visbeck, M. (Eds.), The North Atlantic Oscillation, Climatic Significance
749 and Environmental Impact, AGU Geophysical Monograph, 134, 1–35, 2003.
750 Huth, R., Pokorná, L., Bochníček, J., and Hejda, P.: Combined solar and QBO effects on the
751 modes of low-frequency atmospheric variability in the Northern Hemisphere, Journal of
752 Atmospheric and Solar-Terrestrial Physics, 71(13), 1471-1483, 2009.
753 Ionita, M., Lohmann, G., and Rimbu, N.: Prediction of spring Elbe discharge based on stable
754 teleconnections with winter global temperature and precipitation. Journal of Climate 21,
755 no. 23, 6215-6226, 2008.
756 Landscheidt, T.: River Po discharges and cycles of solar activity. Hydrological Sciences
757 Journal, 45(3), 491-493, 2000.
758 Lejenas, H., and Okland, H.: Characteristics of Northern Hemisphere blocking as determined
759 from a long time series of observational data, Tellus , 35A, 350-362, 1983.
760 Lohmann, G., Rimbu, N., and Dima, M.: Climate signature of solar irradiance variations:
761 analysis of long-term instrumental, historical, and proxy data, International Journal of
762 Climatology, 24(8), pp. 1045-1056, 2004.
763 Lorenzo-Lacruz, J., Vicente Serrano, S. M., López-Moreno, J. I., González-Hidalgo, J.C.,
764 and Morán-Tejeda, E.: The response of Iberian rivers to the North Atlantic Oscillation. 2011.
765 Love, J. J., Mursula, K., Tsai,V. C., and Perkins, D. M.: Are secular correlations between
766 sunspots, geomagnetic activity, and global temperature significant?, Geophys. Res. Lett.,
767 38, L21703, doi: 10.1029/2011GL049380, 2011.
768 Mann, M. E., and Lees, J.: Robust estimation of background noise and signal detection in
769 climatic time series, Climatic Change, 33, 409–445, 1996.
770 Mann, M. E.: On smoothing potentially non-stationary climate time series, Geophys. Res.
771 Lett., 31, L07214, doi: 10.1029/2004GL019569, 2004.
772 Mann, M. E.: Smoothing of climate time series revisited, Geophys. Res. Lett., 35, L16708,
773 doi: 10.1029/2008GL034716, 2008.
774 Mares, I., Mares,C., Mihăilescu,M., Capsună, S., and Chirovici,M.**:** Study of the extreme
775 events in Romania in the regional climate context. International Symposium on Applied
776 Agrometeorology and Agroclimatology, 24-26 April, Volos, Greece, 25-36, 1996.
777 Mares, I., Mares, C., and Mihăilescu, M.: NAO impact on the summer moisture variability
778 across Europe, Physics and chemistry of the Earth, 27, 1013-1017, 2002.
779 Mares, C., Mares, I. and Stanciu, A.: Extreme value analysis in the Danube lower basin
780 discharge time series in the 20 th century, Theoretical and Applied Climatology, 95, 223-
781 233, 2009.
782 Mares, I., Mareş, C. and Mihăilescu M.: On the statistical significance of the sea level
783 pressure climatic signal simulated by general circulation models for the 21 st century over
784 Europe. Rev. Roum. Géophysique, 25–40, 2013a.
785 Mares, I**.**, Mareş, C., and Mihailescu, M.: Stochastic modeling of the connection between sea
786 level pressure and discharge in the Danube lower basin by means of Hidden Markov
787 Model, EGU General Assembly Conference Abstracts, 15, 7606, 2013b.
788 Mares, C., Adler M. J., Mares I, Chelcea, S., Branescu, E.: Discharge variability in Romania
789 using Palmer indices and a simple atmospheric index of large-scale circulation,
790 Hydrological Sciences Journal, doi: 10.1080/02626667.2015.1006233), 2015a.

Mares, I., Dobrica,V., Demetrescu, C., and Mares, C.: Influence of the atmospheric blocking on the hydrometeorological variables from the Danube basin and possible response to the solar/geomagnetic activity, Geophysical Research Abstracts, 17, EGU2015-4154-3,2015, EGU General Assembly 2015 (PICO2.6), 2015b.

Mares, C., Mares, I., and Mihailescu, M.: Identification of extreme events using drought indices and their impact on the Danube lower basin discharge, Hydrological Processes, doi: 10.1002/hyp. 10895), 2016a.

Mares, I., Dobrica, V., Demetrescu, C.,and Mares, C.,: Hydrological response in the Danube lower basin to some internal and external forcing factors of the climate system, Geophysical Research Abstracts, 18, EGU2016-7474, EGU General Assembly 2016b.

Massei, N., Laignel, B., Deloffre, J., Mesquita, J., Motelay, A., Lafite, R., and Durand, A.: Long-term hydrological changes of the Seine River flow (France) and their relation to the North Atlantic Oscillation over the period 1950–2008, International Journal of Climatology, *30*(14), pp.2146-2154, 2010.

Narasimha, R., and Bhattacharyya S. : A wavelet cross-spectral analysis of solar–ENSO–rainfall connections in the Indian monsoons. Applied and Computational Harmonic Analysis 28, no. 3 : 285-295, 2010.

Palamara, D. R., and Bryant, E.A.: March. Geomagnetic activity forcing of the Northern Annular Mode via the stratosphere, in: Annales Geophysicae, 22, No. 3, 725-731, 2004.

Papadimitriou, L. V., Koutroulis, A. G., Grillakis, M. G., and Tsanis, I. K.: High-end climate change impact on European runoff and low flows – exploring the effects of forcing biases, Hydrol, Earth Syst. Sci., 20, 1785-1808, doi:10.5194/hess-20-1785-2016, 2016.

Ped, D. A.: On indicators of droughts and wet conditions (in Russian). Proc. USSR Hydrometeor. Centre, 156, 19–39, 1975.

Peña, J.C., Schulte, L., Badoux, A., Barriendos, M., and Barrera-Escoda, A.: Influence of solar forcing, climate variability and modes of low-frequency atmospheric variability on summer floods in Switzerland. Hydrology and Earth System Sciences, *19*(9), pp.3807-3827, 2015.

Percival, D. B., and Walden, A. T.; Spectral Analysis for Physical Applications, Cambridge University Press, Cambridge, UK., 1986.

Perry, C.A.: Evidence for a physical linkage between galactic cosmic rays and regional climate time series. Advances in Space Research, *40*(3), pp.353-364, 2007.

Press, W. H., Teukolsky, S. A.,Vetterling,W.T., and Flannery, B. P.: Numerical Recipes, Cambridge Univ. Press, Cambridge, U. K., 1992

Prestes, A., Rigozo, N. R., Nordemann, D. J. R., Wrasse, C. M., Echer, M. S., Echer, E., ... and Rampelotto, P. H.: Sun–earth relationship inferred by tree growth rings in conifers from Severiano De Almeida, Southern Brazil, Journal of Atmospheric and Solar-Terrestrial Physics, 73(11), 1587-1593, 2011.

Rai, R. K., Upadhyay, A., Ojha, C. S. P., and Lye L. M.: Statistical analysis of hydro-climatic variables. RY Surampalli, TC Zhang, CSP Ojha, BR Gurjar, RD Tyagi and CM Kao (ed. 2013), Climate change modelling, mitigation, and adaptation. Reston, VA: ASCE. doi 10, no. 9780784412718, 378-388, 2013

Rimbu, N., Boroneanţ, C., Buţă, C., and Dima M.: Decadal variability of the Danube river flow in the lower basin and its relation with the North Atlantic Oscillation, International Journal of Climatology., 22(10):1169-79, 2002.

Rimbu, N., and Lohmann, G.: Winter and summer blocking variability in the North Atlantic region–evidence from long-term observational and proxy data from southwestern Greenland, Climate of the Past, 7(2), 543-555, 2011.

Rimbu, N., Dima, M., Lohmann, G. and Musat, I.: Seasonal prediction of Danube flow variability based on stable teleconnection with sea surface temperature, Geophysical Research Letters, 32(21), 2005.

Scaife, A. A., Ineson, S., Knight, J. R., Gray, L.J., Kodera, K., and Smith, D. M.: A mechanism for lagged North Atlantic climate response to solar variability, Geophys. Res. Letts., 40, 434–439, doi:10.1002/grl.50099, 2013.

Sfîcă, L., Voiculescu, M., and Huth, R.: The influence of solar activity on action centres of atmospheric circulation in North Atlantic, Ann. Geophys., 33, 207-215, doi:10.5194/angeo-33-207-2015, 2015.

Sunkara, S. L. and Tiwari, R. K.: Wavelet analysis of the singular spectral reconstructed time series to study the imprints of solar–ENSO–geomagnetic activity on Indian climate, Nonlin. Processes Geophys., 23, 361-374, doi:10.5194/npg-23-361-2016, 2016.

Tapping, K.F. : The 10.7 cm solar radio flux (F10. 7), Space Weather, 11(7), 394-406, 2013.

Thiebaux, H. J., and Zwiers, F. W.: The interpretation and estimation of effective sample size, J. Climate Appl. Meteor., 23**,** 800–811, 1984.

Thiéblemont, R., Matthes, K., Omrani, N-E. Kodera, K., and Hansen,F. : Solar forcing synchronizes decadal North Atlantic climate variability. Nature communications 6, 2015.

Thomson, D. J.: Spectrum estimation and harmonic analysis, IEEE Proc.,70, 1055-1096, 1982.

Tomasino, M., and Valle, F. D. : Natural climatic changes and solar cycles: an analysis of hydrological time series. Hydrological sciences journal, 45(3), 477-489, 2000.

Torrence, C., and Compo, G. P.: A practical guide to wavelet analysis. Bull. Amer. Meteor. Soc., 79**, 61**–78, 1998.

Trenberth, K. E., and Paolino, D. A.: The Northern Hemisphere sea level pressure data set: Trends, errors, and discontinuities, Mon. Weather Rev. 108: 855-872, 1980.

Turki, I., Laignel, B., Massei, N., Nouaceur, Z., Benhamiche, N., and Madani, K.: Hydrological variability of the Soummam watershed (Northeastern Algeria) and the possible links to climate fluctuations, Arabian Journal of Geosciences, 9(6), 1-12, 2016.

Valty, P., De Viron, O., Panet, I., and Collilieux, X.,: Impact of the North Atlantic Oscillation on Southern Europe Water Distribution: Insights from Geodetic Data. Earth Interactions, 19 (10), 1-16, 2015.

Van Loon H. and Labitzke, K: Association between the 11-Year Solar Cycle, the QBO, and the Atmosphere. Part II: Surface and 700 mb in the Northern Hemisphere in Winter, J. Climate, 1, 905–920, 1988.

Van Loon, H., and Meehl, G. A.: Interactions between externally forced climate signals from sunspot peaks and the internally generated Pacific Decadal and North Atlantic Oscillations, Geophys.Res. Lett., 41, 161–166, doi:10.1002/ 2013GL058670, 2014.

Velasco, V. M., and Mendoza B. : Assessing the relationship between solar activity and some large scale climatic phenomena. Advances in Space Research 42, no. 5, 866-878,.2008.

Versteegh, G.J.M.: Solar forcing of climate. 2: Evidence from the past. Space Sci. Rev. 120, 243–286, 2005.

Vlasov, A., Kauristie, K., Kamp, M., Luntama, J.P. and Pogoreltsev, A.: A study of traveling ionospheric disturbances and atmospheric gravity waves using EISCAT Svalbard Radar IPY-data. Annales Geophysicae, 29, No. 11, 2101-2116). Copernicus GmbH, 2011.

Von Storch H.V. and Zwiers F. W.: Statistical Analysis in Climate Research. Cambridge University Press, 484, 1999.

Wang, J. S., and Zhao, L.: Statistical tests for a correlation between decadal variation in June precipitation in China and sunspot number, J. Geophys. Res., 117, D23117, doi:10.1029/2012JD018074, 2012.

Zanchettin, D., Rubino, A., Traverso, P., and Tomasino, M. : Impact of variations in solar activity on hydrological decadal patterns in northern Italy, J. Geophys. Res., 113, D12102, doi: 10.1029/2007JD009157, 2008.

Zwiers, F. W., and von Storch H: Taking Serial Correlation into Account in Tests of the Mean. J. Climate, 8, 336-351, 1995

Table 1. Correlation coefficient between first principal component (PC1) for the precipitation and atmospheric indices NAO and GBO, during winter

Period	NAOI	GBOI
1916-1957	-0.36	**0.75**
1958-1999	**-0.43**	**0.84**

Table 2. Simultaneous correlation (1901-2000) with confidence level (CL) at least 95%, for unfiltered (UF) data, terrestrial variables filtered by low pass filter (LPF) and both time series correlated, smoothed by band pass filtered and the band is specified in the brackets. *r*- Pearson correlation coefficient, *t*- the values of test *t*, τ - Kendall correlation coefficient, p - significance p-level, N_{eff} is the effective number.

Variable	*Season*	*r*	*t*	τ	*p*	N_{eff}	*CL*
Correlation with aa							
PC1_TT(UF)	**Spring**	**0.224**	**2.184**	**0.137**	**0.043**	**92**	**95%**
PC1_TT(4-8)	**Spring**	**0.606**	**6.457**	**0.401**	**0.000**	**74**	**99.5%**
PC1_TT(UF)	**Summer**	**0.310**	**2.663**	**0,206**	**0.002**	**69**	**99%**
PC1_TT(LPF)	**Summer**	**0.345**	**2.037**	**0.210**	**0.002**	**33**	**95%**
PC1_TT(9-15)	**Summer**	**0.796**	**5.130**	**0.570**	**0.000**	**17**	**99.5%**
PC1_TT(LPF)	Fall	0.453	2.865	0.304	0.000	34	99%
PC1_PP(LPF)	**Spring**	**-0.371**	**2.201**	**-0.315**	**0.000**	**32**	**95%**
PC1_PP(9-15)	**Spring**	**-0.669**	**3.437**	**-0.501**	**0.000**	**17**	**99.5%**
PC1_PP(9-15)	Summer	-0.721	3.910	-0.523	0.000	16	99.5%
TPPI(LPF)	Fall	0.452	2.869	0.310	0.000	34	99%
TPPI(UF)	**Spring**	**0.275**	**2.676**	**0.186**	**0.006**	**90**	**99%**
TPPI(LPF)	**Spring**	**0.299**	**1.736**	**0.261**	**0.000**	**33**	**90%**
TPPI(4-8)	**Spring**	**0.525**	**5.313**	**0.338**	**0.000**	**76**	**99.5%**
TPPI(9-15)	**Spring**	**0.402**	**1.660**	**0.325**	**0.000**	**16**	**85-90%**
TPPI(UF)	**Summer**	**0.224**	**2.121**	**0.153**	**0.025**	**87**	**95%**
TPPI(LPF)	**Summer**	**0.318**	**1.921**	**0.187**	**0.006**	**35**	**~95%**
TPPI(9-15)	**Summer**	**0.787**	**4.856**	**0.572**	**0.000**	**16**	**99.5%**
ORS_Q(LPF)	**Fall**	**-0.324**	**1.946**	**-0.210**	**0.002**	**34**	**~95%**
ORS_Q(9-15)	**Fall**	**-0.562**	**2.454**	**-0.419**	**0.000**	**15**	**95-98%**
ORS_Q(9-15)	Summer	-0.656	3.210	-0.470	0.000	16	99%
Correlation with Wolf number							
PC1_TT(4-8)	Summer	0.288	2.453	0.157	0.021	68	98%
PC1_TT(9-15)	Fall	0.699	3.770	0.550	0.000	17	99.5%
PC1_PP(4-8)	**Spring**	**-0.242**	**2.133**	**-0.190**	**0.005**	**75**	**95-98%**
PC1_PP(9-15)	**Spring**	**-0.538**	**2.417**	**-0.363**	**0.000**	**16**	**95-98%**
PC1_PP(4-8)	Winter	-0.370	3.298	-0.265	0.000	70	>99%

TPPI(UF)	**Spring**	**0.211**	**1.973**	**0.148**	**0.029**	**85**	**95%**
TPPI(LPF)	**Spring**	**0.299**	**1.736**	**0.261**	**0.000**	**33**	**90%**
TPPI(4-8)	**Spring**	**0.245**	**2.154**	**0.159**	**0.019**	**74**	**95-98%**
TPPI(9-15)	**Spring**	**0.585**	**2.708**	**0.395**	**0.000**	**16**	**98%**
TPPI(9-15)	Fall	0.673	3.796	0.553	0.000	19	99%
GBOI (4-8)	Summer	-0.346	2.982	-0.230	0.001	67	99.5%
GBOI (4-8)	Winter	-0.343	3.169	-0.218	0.001	77	>99%
GBOI (17-28)	Fall	-0.899	3.485	-0.707	0.000	5	95-98%
ORS_Q (4-8)	Winter	-0.263	2.329	-0.163	0.016	75	98%

Table 3. Same as Table 2 but for 53 years (1948-2000).

Variable	*Season*	*r*	*t*	τ	*p*	N_{eff}	*CL*
Correlation with aa							
EBI (UF)	**Spring**	**0.259**	**1.836**	**0.151**	**0.110**	**49**	**~95%**
EBI (4-8)	**Spring**	**0.528**	**3.864**	**0.382**	**0.000**	**41**	**>99%**
ABI (UF)	Fall	-0.257	1.848	-0.118	0.210	51	~95%
ABI (9-15)	Spring	0.605	2.157	0.426	0.000	10	>95%
AEBI (9-15)	Winter	0.749	3.134	0.589	0.000	10	98.5%
Correlation with flux 10.7 cm							
TPPI(LPF)	Spring	0.444	1.502	0.322	0.001	11	85-90%
ABI(4-8)	Fall	0.578	4.124	0.312	0.001	36	99.9%
AEBI(4-8)	Fall	0.530	3.697	0.360	0.000	37	99.9%
EBI (4-8)	**Winter**	**0.419**	**2.678**	**0.272**	**0.004**	**37**	**98.5%**
ORS_Q(4-8)	**Winter**	**-0.603**	**4.390**	**-0.351**	**0.000**	**36**	**99.9%**
GBOI (4-8)	**Winter**	**-0.695**	**6.034**	**-0.428**	**0.000**	**41**	**99.9%**

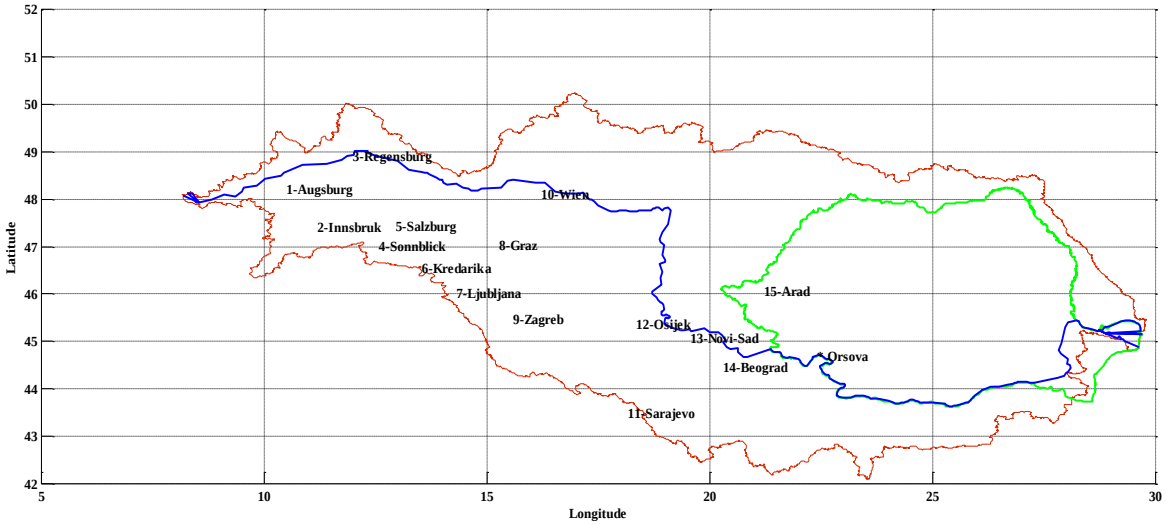

Figure 1. Localization of 15 precipitation stations situated upstream of Orsova station.

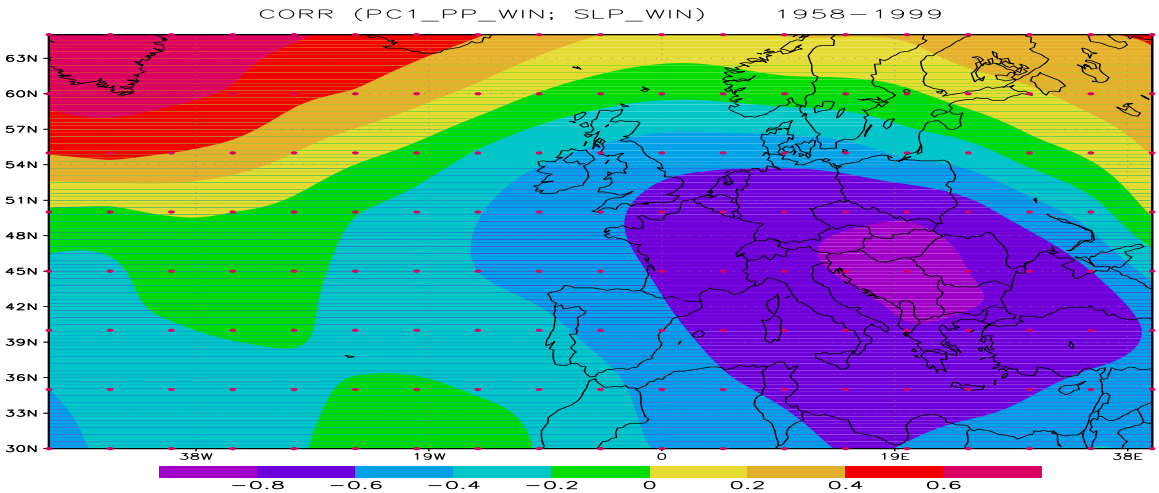

Figure 2. Spatial distribution of correlation coefficients between SLP NCAR and observed PC1- PP during winter for 1958-1999.

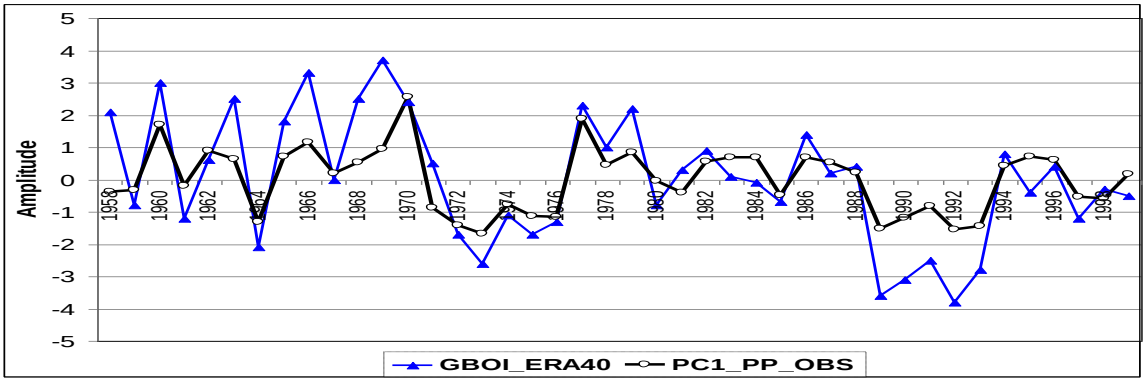

Figure 3. Winter precipitation PC1 versus winter GBOI for 1958-1999 **(R=0.84).**

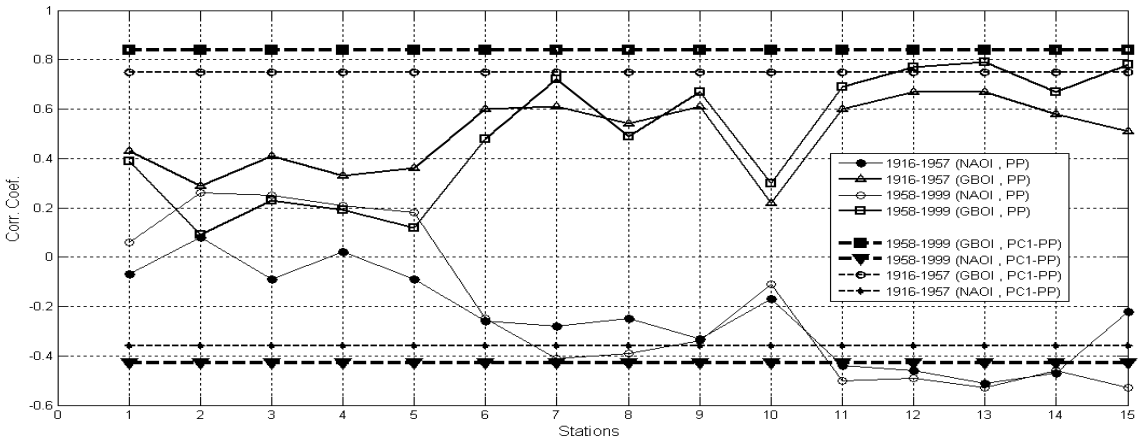

Figure 4. Correlation coefficients between winter precipitation at 15 stations and NAOI and GBOI for two periods: a) 1916-1957; b) 1958-1999. The correlations between PC1-PP and two indices are marked by horizontal lines.

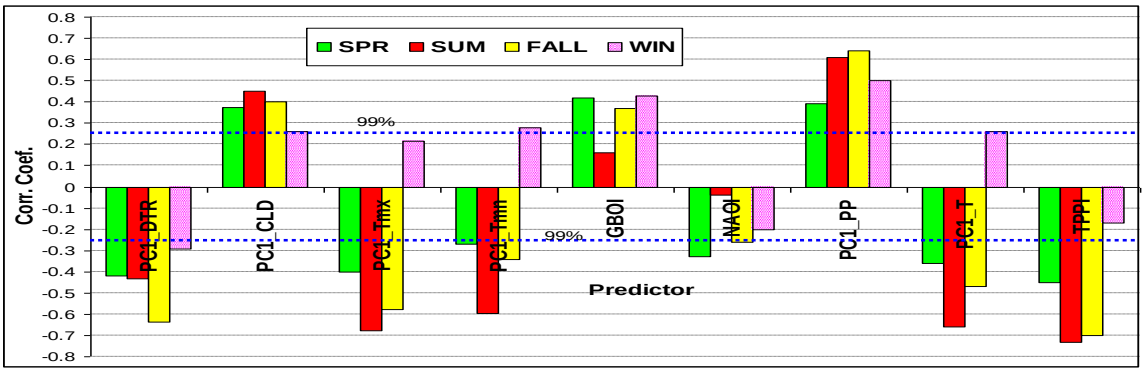

Figure 5. Simultaneous correlations (1901-2000) between Danube discharge at Orsova and nine predictors: diurnal temperature range (DTR), cloud cover (CLD), maximum and minimum temperatures (Tmx, Tmn), atmospheric indices GBOI and NAOI, precipitation (PP), mean temperature (T) and drought index (TPPI). PC1 represents the first principal components of the respective fields.

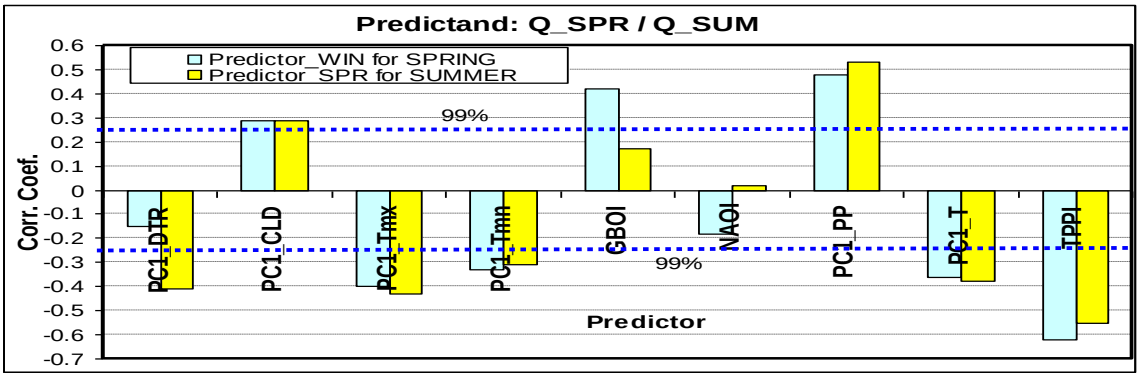

Figure 6. The correlation between Orsova discharge (Q) in the spring / summer and the nine predictors in the winter/spring.

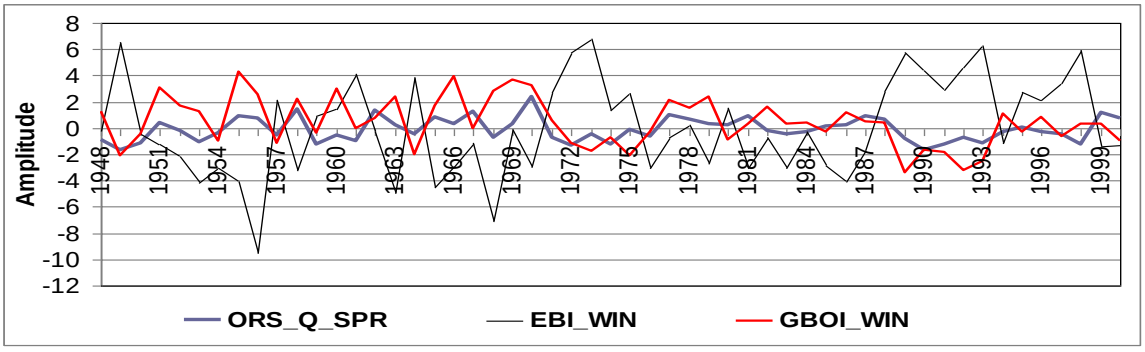

Figure 7. Spring Orsova discharge (standardized) versus winter European blocking index (R= - 0.54) and winter GBOI (R=0.53) for the period 1948-2000.

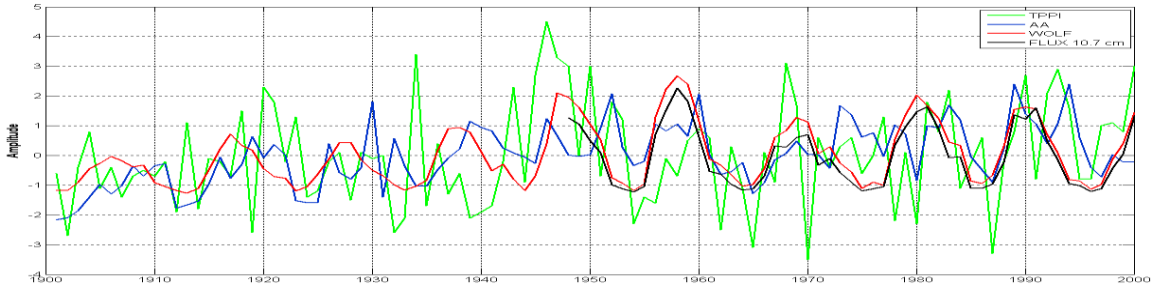

Figure 8. Unfiltered spring **t**ime series of Wolf number, *aa*, and TPPI for the period 1901-2000 and solar flux since 1948. The time series are standardized except for TPPI.

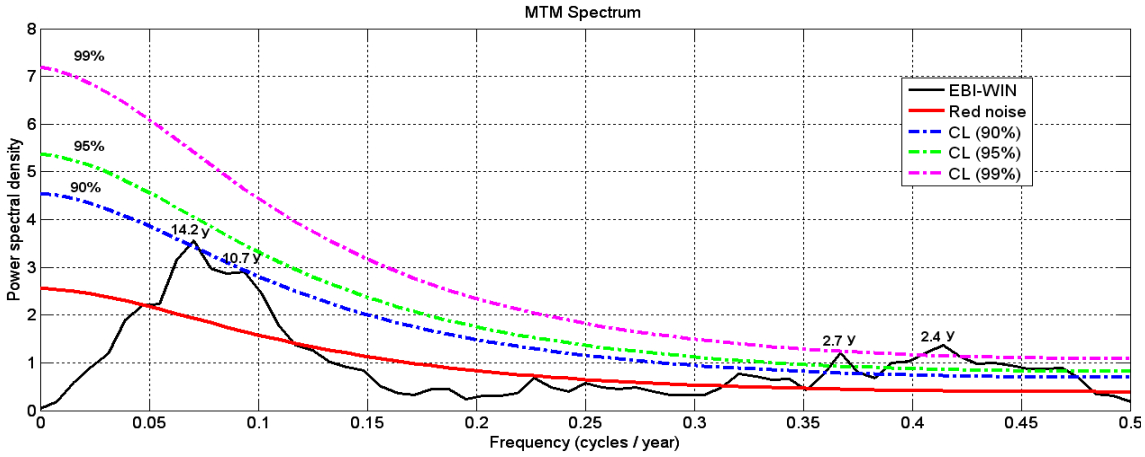

a)

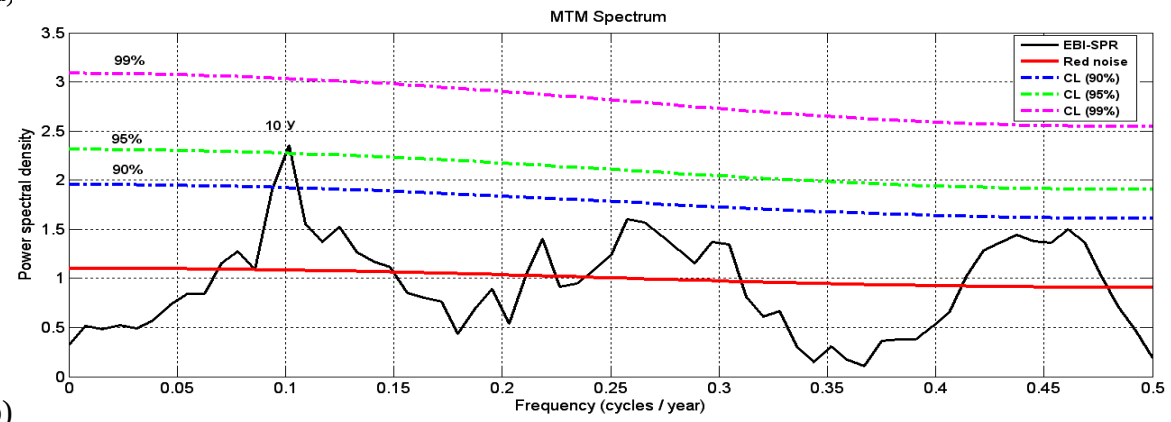

b)

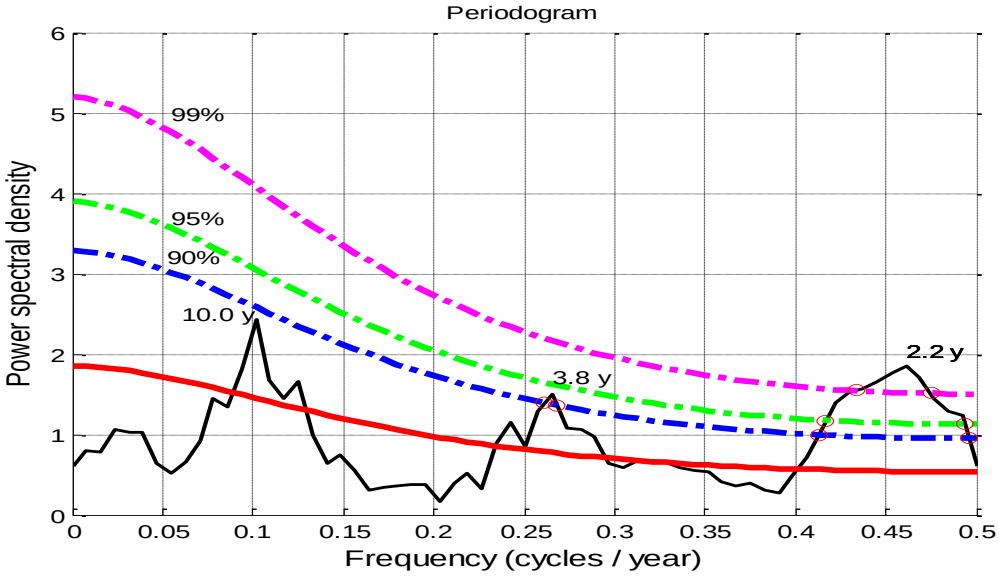

c)

Figure 9. Power spectra for the blocking indices: winter EBI (a), spring EBI (b) and spring AEBI (c).

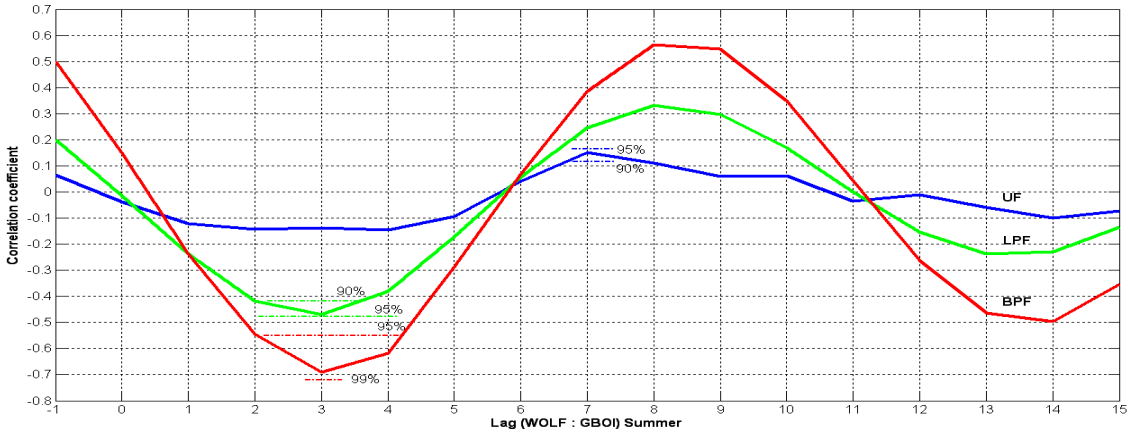

Figure 10. Correlation coefficients, between Wolf number and GBOI in summer with the lags between -1 and 15 yr, for three time series: unfiltered (UF), smoothing by low pass filter (LPF) and by band pass filter (9-15). The Wolf number is considered before GBOI, from 1 to 15yr.

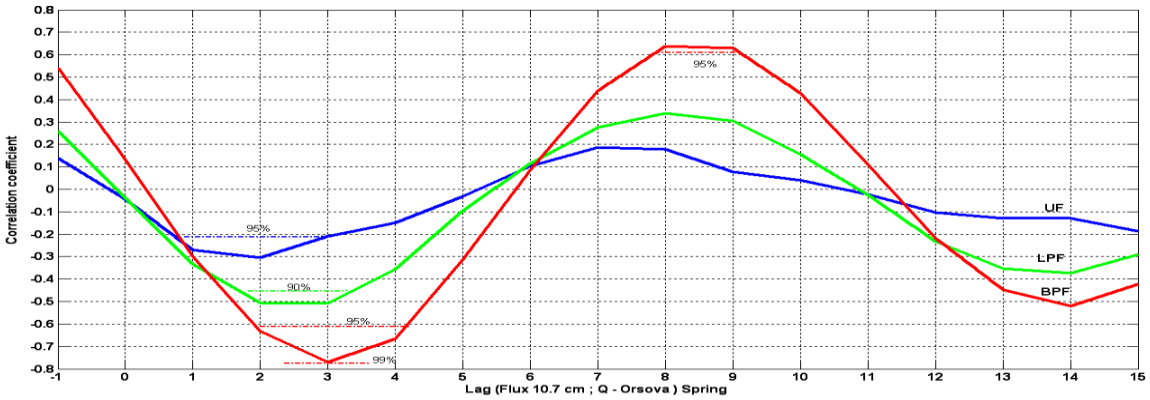

a)

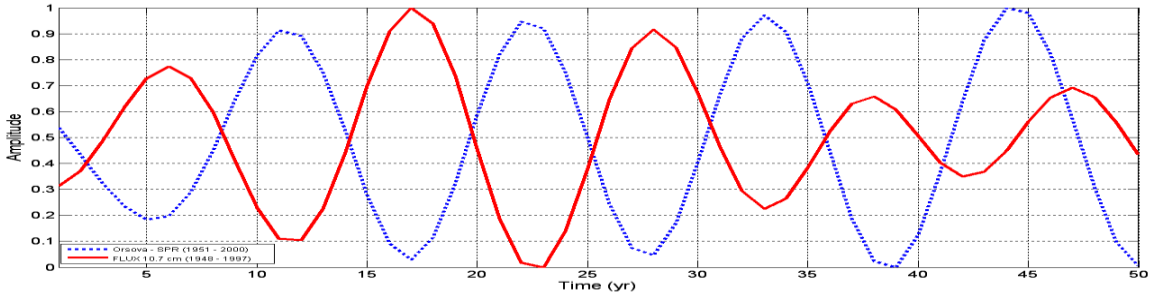

b)

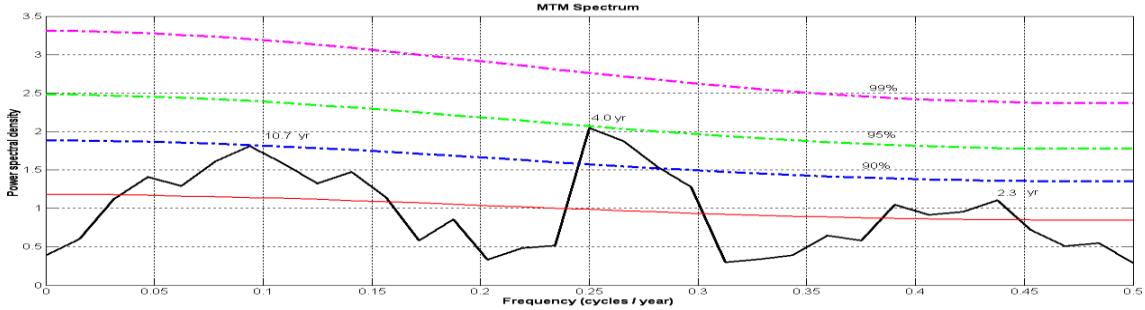

c)

Figure 11. The test of a possible association between solar (Flux 10.7cm) and the Orsova dischage (ORS_Q), during spring (1948-2000).

a) Correlation coefficients, between solar flux and Orsova discharge with the lags from -1 to 15 yr, for three time series: unfiltered (UF), smoothing by low pass filter (LPF) and by band pass filter (9-15);
b) Temporal behavior of the solar flux and ORS_Q, filtered (9-15) with a delay of 3 years to flux. The time series are normalized.
c) Power spectra for spring discharge at Orsova. The time series is unfiltered.

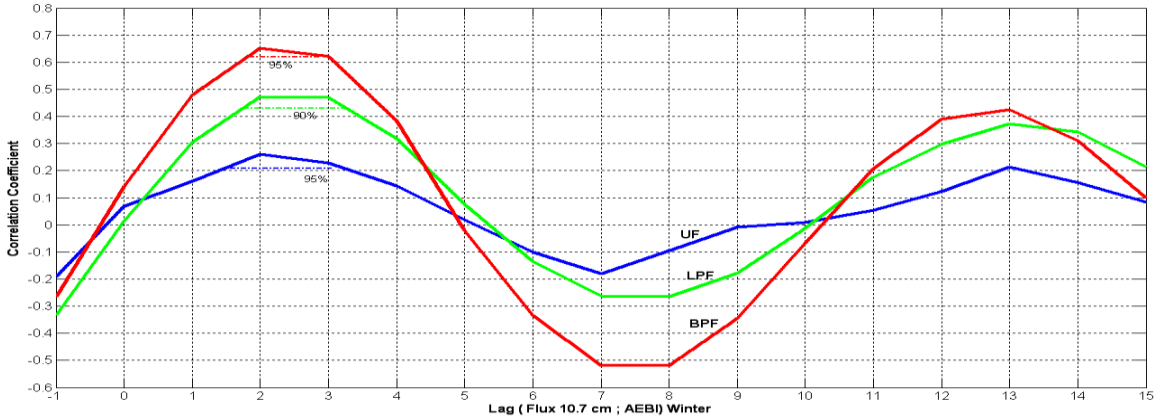

Figure 12. Correlation coefficients, between solar flux and AEBI with the lags between -1 and to 15yr, during winter (1948-2000), for three time series: unfiltered (UF), smoothing by low pass filter (LPF) and by band pass filter (9-15).

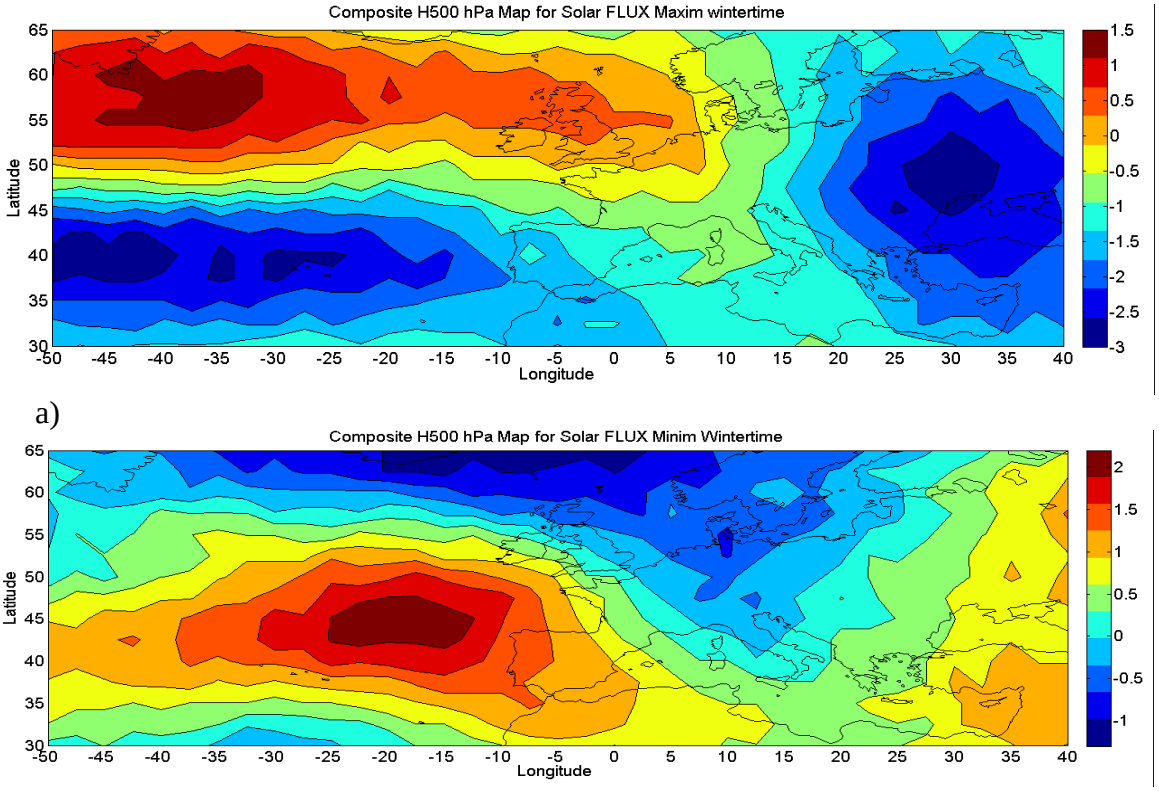

Figure 13. Composite maps for the winter H500 hPa anomalies, corresponding to solar flux associated with the east phase of QBO (1948-2000) and: a) maximum flux b) minimum flux